Ceramics International 44 (2018) 9097–9104

Contents lists available at ScienceDirect

Ceramics International

journal homepage: www.elsevier.com/locate/ceramint

Magnesium ferrite nanoparticles as a magnetic sorbent for the removal of Mn^{2+}, Co^{2+}, Ni^{2+} and Cu^{2+} from aqueous solution

A.I. Ivanets[a,*], V. Srivastava[b], M.Yu. Roshchina[a], M. Sillanpää[b,c], V.G. Prozorovich[a], V.V. Pankov[d]

[a] Institute of General and Inorganic Chemistry of National Academy of Sciences of Belarus, st. Surganova 9/1, 220072 Minsk, Belarus
[b] Laboratory of Green Chemistry, Lappeenranta University of Technology, Sammonkatu 12, 50130 Mikkeli, Finland
[c] Department of Civil and Environmental Engineering, Florida International University, Miami FL-33174, USA
[d] Department of Physical Chemistry, Belarusian State University, Leningradskaya St. 14, 220050 Minsk, Belarus

ARTICLE INFO

Keywords:
Magnetic sorbent
$MgFe_2O_4$ nanoparticles
Isotherm modeling
Metal ions
Wastewater treatment

ABSTRACT

The aim of this research was to prepare magnesium ferrite ($MgFe_2O_4$) magnetic nanoparticles and to investigate their sorption characteristics towards Mn^{2+}, Co^{2+}, Ni^{2+}, Cu^{2+} ions in aqueous solution. $MgFe_2O_4$ was synthesized by glycine-nitrate combustion method and was characterized by low crystallinity with crystallite size of 8.2 nm, particle aggregates of 13–25 nm, BET surface area of 14 m^2/g and pore size of 8.0 nm. Sorption properties of $MgFe_2O_4$ towards Mn^{2+}, Co^{2+}, Ni^{2+}, Cu^{2+} ions were studied using one-component model solutions and found to be dependent on metal ions concentration, contact time, pH and conditions of regeneration experiment. The highest sorption capacity of $MgFe_2O_4$ was detected towards Co^{2+} (2.30 mmol g^1) and Mn^{2+} (1.56 mmol g^{-1}) and the lowest towards Ni^{2+} (0.89 mmol g^{-1}) and Cu^{2+} (0.46 mmol g^{-1}). It was observed that sorption equilibrium occurs very quickly within 20–60 min. The pH_{zpc} of sorbent was calculated to be 6.58. At studied pH interval (3.0–7.0) the sorption capacity of $MgFe_2O_4$ was not significantly affected. Regeneration study showed that the metal loaded sorbent could be regenerated by aqueous solution of 10^{-3} M $MgCl_2$ at pH 6.0 within 120 min of contact time. Regeneration test suggested that $MgFe_2O_4$ magnetic sorbent can be efficiently used at least for four adsorption-desorption cycles. The high sorption properties and kinetics of toxic metal ion sorption indicates good prospects of developed sorbent in practice for wastewater treatment.

1. Introduction

Water pollution by toxic compounds (heavy metal ions, radionuclides, dyes, pharmaceutical substance, etc.) is one of the most important contemporary problems of environmental protection [1–3]. Due to high efficiency, experimental simplicity and low operating costs, sorption method is widely used for the purification of water media from a variety of pollutants [4,5]. In addition to the high sorption capacity and kinetics, the adsorbents should be easily separable from the purified solutions and regenerated for multiple use [6].

Due to various advantages of sorption method, the great attention of researchers is paid to the development of magnetic sorbents, which can be easily separated from aqueous media via magnetic separation and do not require the use of decantation, centrifugation, membrane filtration and other methods [7–11]. Typically, such materials include composites of magnetite (Fe_3O_4) with silica [12], clay materials [13], natural and synthetic zeolites [14,15], carbon materials (activated carbon, carbon nanotubes, graphene, graphene oxide) [16,17], metal oxides (Al_2O_3, MnO_2, TiO_2, etc.) [18–20] and hydroxides [21] and other sorbents.

Metal ferrites $M^{2+}Fe_2^{3+}O_4$ (M: Mg^{2+}, Mn^{2+}, Co^{2+}, Ni^{2+}, Cu^{2+}, Zn^{2+}, etc.) due to their high stability, high surface area and excellent magnetic characteristics are more attractive for sorption processes in comparison to Fe_3O_4 composites. Metal ferrites with a spinel structure are crystallized in a cubic lattice with *Fd3m*, Z = 8 space group, in which the cations are located in octahedral and tetrahedral lattice sites. Recent review papers [22,23] showed that this class of materials are effective sorbents for the purification of aqueous solutions from a wide range of pollutants, described approaches to their synthesis using green chemistry methods, and demonstrated the possibility of regeneration and approaches to the disposal of used materials.

It is important to note that one of the drawbacks of most transition metal ferrites is a partial leaching of toxic metals (Mn^{2+}, Co^{2+}, Ni^{2+}, Cu^{2+}, etc.) in solution during treatment process, which often leads to secondary pollution [24]. In addition, for the regeneration of these sorbents after the sorption of metal ions, use of solutions of various acids (HCl, H_2SO_4, CH_3COOH, etc.) is proposed. This causes the formation of acidic wastewater that requires subsequent neutralization

* Corresponding author.
E-mail address: Ivanets@igic.bas-net.by (A.I. Ivanets).

https://doi.org/10.1016/j.ceramint.2018.02.117
Received 24 January 2018; Received in revised form 12 February 2018; Accepted 12 February 2018
Available online 13 February 2018
0272-8842/

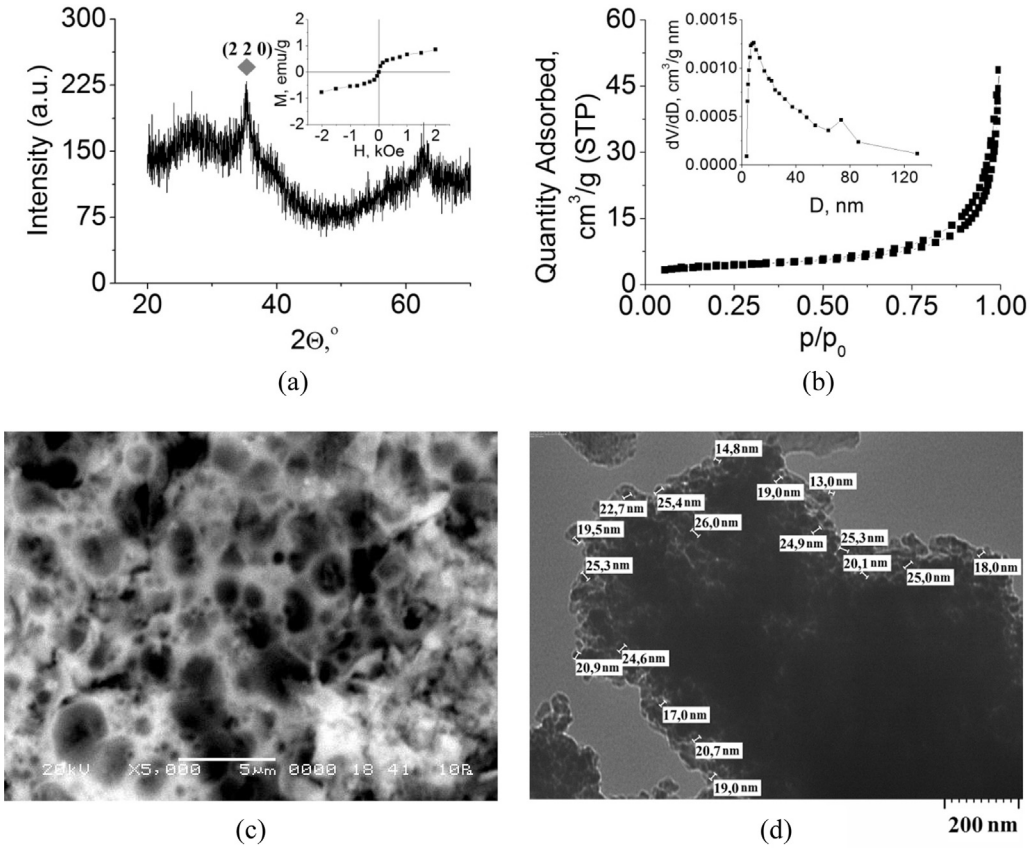

Fig. 1. XRD patterns and magnetization hysteresis at room temperature (a), isotherms of N_2 adsorption-desorption and distribution of the pore diameters (b), SEM image, magnitude × 5000 (c) and TEM image, magnitude ×50000 (d) of $MgFe_2O_4$ sorbent.

before their disposal [25].

In the present work, magnetic $MgFe_2O_4$ nanoparticles were obtained using glycine-nitrate method and were characterized by XRD, SEM, TEM and adsorption-desorption of nitrogen. The choice of this object of study is due to the safety of materials for humans and living organisms in contrast to ferrites of transition metals. The aim of the work was to study the sorption characteristics of $MgFe_2O_4$ magnetic nanoparticles towards Mn^{2+}, Co^{2+}, Ni^{2+} and Cu^{2+} ions from one-component aqueous solutions and dependence on various factors (initial concentration of metal ions, contact time, pH and regeneration conditions).

2. Materials and methods

2.1. Chemicals

For $MgFe_2O_4$ sorbent synthesis, the chemicals $Mg(NO_3)_2$, $Fe(NO_3)_3$, NaCl, $C_2H_5NO_2$ of analytical grade purchased from " 5 Oceans" (Belarus) were used. For aqueous model solutions preparation, metal chlorides ($MnCl_2$, $CoCl_2$, $NiCl_2$, $CuCl_2$, $MgCl_2$) purchased from Sigma Aldrich were used without additional purification.

2.2. Synthesis of magnesium ferrite

Sorbent magnesium ferrite nanoparticles was obtained using glycine-nitrate synthesis method. The metal nitrates were mixed in a molar ratio of Mg^{2+}:Fe^{3+} = 1:2. Further, at room temperature (21 ± 1 °C) relative to the product, inert component NaCl was injected in the resulting solution in a weight ratio of 10:1. NaCl, which acted as a high temperature solvent to create "protected" and not aggregated nanoparticles.

In similar conditions glycine (H_2NCH_2COOH) was added into the resulting solution, at a molar ratio of 4:1 with respect to a product, which acted as a complexing agent and a reducing agent. The resulting mixture was stirred and evaporated at 80 °C for 1 h until the formation of a viscous gel. Further, heating of the gel mass resulted in its spontaneous combustion with the formation of combustion products consisting of oxide mixture, coal and NaCl. The resulting mixture was heated in a muffle furnace at 300 °C for 5 h. Magnesium ferrite nanoparticles were separated from the matrix NaCl by magnetic separation and washed repeatedly by distilled water.

2.3. Sorbent characterization methods

To determine the phase composition of the obtained magnesium ferrite, as well as to calculate the '*a*' parameter of the crystal lattice and to estimate the crystallite sizes by Scherrer formula [26], XRD analysis was performed on a D8 ADVANCE diffractometer (Bruker, Germany).

The surface morphology and particle size were studied using scanning electron microscopy (SEM) by JSM-5610 LV (JEOL, Japan) and transmittance electron microscopy (TEM) by HITACHI 7700 operated at 100 kV. For TEM analysis of sample, the $MgFe_2O_4$ particles were dispersed in ethanol followed by 20 min sonication to get suspensions of dispersed particles. Further, a drop of suspension were deposited on the carbon-coated copper grids (3 nm Carbon film, 400 Mesh) and then TEM images were collected at 50 K magnifications.

The adsorption properties and the texture of the samples were evaluated from the low temperature physical nitrogen adsorption–desorption isotherms (-196 °C) and the surface area and porosity measured using the volumetric method on a BET analyzer (Model: Micrometritics-Tristar® II Plus). The pore surface area per unit mass of the solid material (specific surface area) was determined using the BET method (A_{BET}). The adsorption pore volume ($V_{sp.ads}$) and adsorption mean pore diameter ($D_{sp.ads}$) were calculated using the single point

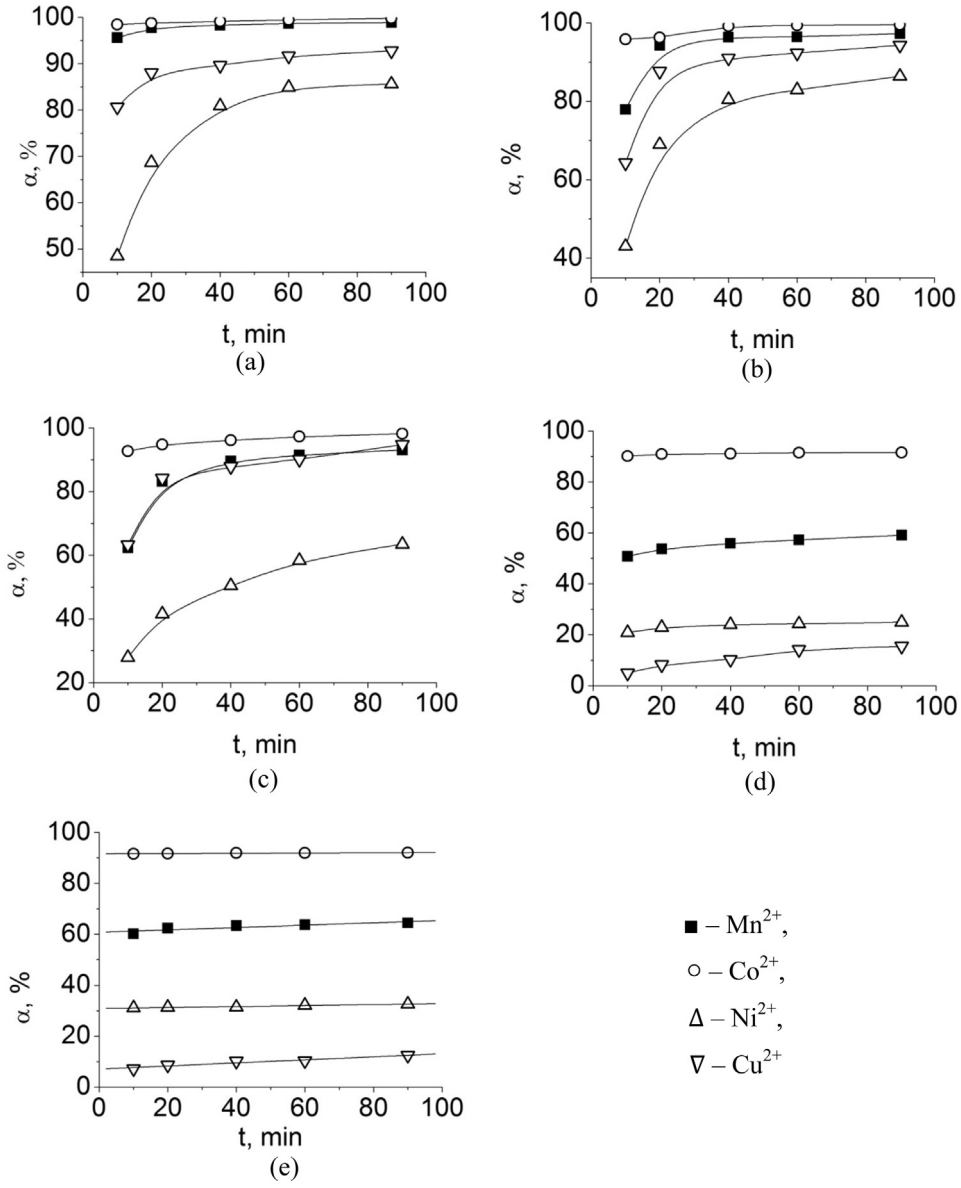

Fig. 2. Effect of contact time and initial metal ions concentrations on removal efficiency from model solutions at pH = 5.0: 10^{-4} M (a), 5×10^{-4} M (b), 10^{-3} M (c), 5×10^{-3} M (d), 10^{-2} M (e).

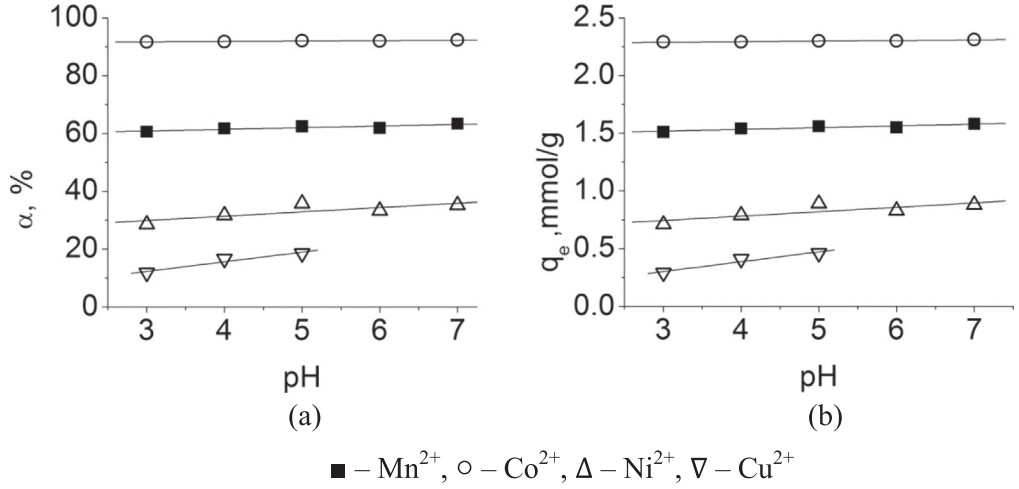

Fig. 3. Effect of pH on (a) metal ions removal efficiency and (b) sorption capacity. Initial metal ions concentration C_0 = 0,01M and contact time – 120 min.

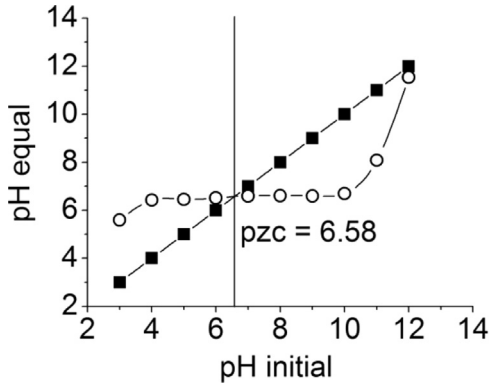

Fig. 4. Plot of $pH_{eq.}$ *vs* $pH_{init.}$ for $MgFe_2O_4$ sample.

method. The adsorption cumulative pore surface area with a diameter of 1.7–300 nm (A_{BJHads}), adsorption cumulative pore volume (V_{BJHads}) with a diameter from the same range, mean adsorption pore diameter (D_{BJHads}), and differential distribution of the mesopore volume over diameters (*dV/dlogD*) were calculated using the Barrett–Joyner–Halenda (BJH) method.

2.4. Sorption experiments

The concentration of metal ions in model solutions was determined using the method of optical emission spectrometry with inductively coupled plasma optical emission spectrometer (ICP-OES 5110 Agilent Technologies). pH of aqueous solutions was measured using pH-meter 340i (± 0,02) (Mettler Toledo, USA).

To study the effect of metal ion concentration and contact time of sorbent with solution, 0.04 g $MgFe_2O_4$ sorbent was kept in 10.0 mL aliquot of model solution (V/m = 250 mg L^{-1}; pH = 5.0) with metal ion concentrations (Mn^{2+}, Co^{2+}, Ni^{2+}, Cu^{2+}) of 10^{-4}, 10^{-3} 10^{-2} M. Samples were taken after 10, 20, 40, 60, and 90 min of contact time with sorbent and were analyzed using ICP-OES.

The influence of pH on efficiency of sorbent for Mn^{2+}, Co^{2+}, Ni^{2+} and Cu^{2+} ion removal from the solution was carried out in the range of 3.0 and 7.0 by keeping 0.04 g $MgFe_2O_4$ in the aliquot of 10.0 mL of the model solution with a concentration of 0.01 M metal ions (V/m = 250 mg L^{-1}) for 120 min. Study of the Cu^{2+} ion sorption was carried out in the pH range of 3.0–5.0 to avoid the formation of the insoluble hydroxide at higher pH values. After sorption, the $MgFe_2O_4$ nanoparticles was separated from the solution by centrifugation at 5000 rpm for 3 min and the solution was analyzed using ICP-OES for remaining metal ion concentration in aliquot.

To determine the pH of point of zero charge (pH_{pzc}) charge, 0.04 g $MgFe_2O_4$ was placed in an aliquot of 10.0 mL (V/m = 250 mg L^{-1}) 0.01 M NaCl solution in the pH range of 3.0–12.0 and was stirred for 48 h. Then sorbent was separated from solution and the equilibrium pH value was measured. Sorption capacity (q_e, mmol g^{-1}) and the removal efficiency (α, %) were calculated using the following equations:

$$q_e = \left(\frac{C_0 - C_e}{m}\right) \cdot V \quad (1)$$

$$\alpha = \frac{(C_0 - C_e) \cdot 100}{C_e} \quad (2)$$

Where m is the sorbent mass (g), V – volume of solution (L), C_0 and C_e – initial and equilibrium concentrations (mmol g^{-1}), respectively.

To study the isotherms of Mn^{2+}, Co^{2+}, Ni^{2+}, Cu^{2+} sorption 0.04 g of $MgFe_2O_4$ was placed in an aliquot of 10.0 mL (V/m = 250 mL g^{-1}) solution of the appropriate metal with an initial concentration in the range of 10^{-4}–10^{-2} M. For all solutions, the initial pH value was adjusted to 5.0 and contact time of sorbent with solutions was 120 min. Then sorbent was separated by centrifugation at 5000 rpm for 3 min, the resulting solution was analyzed on ICP-OES. For the analysis of sorption isotherms, the well known Langmuir (Eq. (3)), Freundlich (Eq. (5)), Sips (Eq. (6)) and Redlich-Peterson (Eq. (7)) models were used.

$$q_e = \frac{q_m K_L C_e}{1 + K_L C_e} \quad (3)$$

Where q_e is the sorption capacity (mmol g^{-1}), C_e – equilibrium concentration (mmol L^{-1}), q_m – maximum sorption capacity (mmol g^{-1}), K_L – coefficient describing affinity of the adsorbate to the adsorbent, (L mmol $^{-1}$).

If experimental data are adequately described by the Langmuir equation, the equilibrium parameter R_L can be calculated by following Eq. (4) [27].

$$R_L = \frac{1}{1 + K_L C_0} \quad (4)$$

Where R_L is the equilibrium parameter.

$$q_e = K_F C_e^{1/n_F} \quad (5)$$

Where K_F ((mmol g^{-1})/(L mmol $^{-1}$)$^{n}_{F}$) is Freundlich constant; n_F – Freundlich exponent.

$$q_e = \frac{K_S q_m C_e^{1/n_S}}{1 + K_S C_e^{1/n_S}} \quad (6)$$

Where is K_S – Sips constant ((mmol L^{-1})$_S^{-1/n}$); n_S – Sips exponent ($0 < n_S \leq 1$).

$$q_e = \frac{K_{RP} C_e}{1 + a_{RP} C_e^{g}} \quad (7)$$

Where is K_{RP} – Redlich-Peterson constant (L mmol $^{-1}$); a_{RP} – Redlich-Peterson constant ((mmol L^{-1})$^{-g}$); g – Redlich-Peterson constant ($0 < g \leq 1$).

2.5. Sorbent regeneration

$MgCl_2$ solutions with concentrations of 10^{-3}, 10^{-2} and 10^{-1} M were used for the regeneration of $MgFe_2O_4$ after sorption of metal ions. A portion (0.02 g) of the sorbent obtained after adsorption from 10^{-2} M solutions of Mn^{2+}, Co^{2+}, Ni^{2+} and Cu^{2+} (V/m = 250 mL g^{-1}, pH = 5.0, contact time 120 min) was kept in the aliquot of 10.0 mL (V/m = 500 mL g^{-1}) of a solution of $MgCl_2$, at pH = 6.0 for 120 min. After separation of the sorbent from the regeneration solution by centrifugation, the sample was dried in air at 80 °C and was again used for the sorption of metal ions in the same conditions. To determine the effectiveness of sorbent regeneration, four cycles of sorption-desorption were conducted using 10^{-3} M solution of $MgCl_2$.

3. Results and discussion

3.1. $MgFe_2O_4$ nanoparticles characterization

According to the XRD data (Fig. 1a), the synthesized sorbent is a magnesium ferrite $MgFe_2O_4$ with a low degree of crystallinity. The *a* parameter of the crystal lattice is 8.393 Å, which is slightly different from the reference value of 8.370 Å and due to the disorder and lattice defects of the crystalline structure of the investigated sorbent. The size of the crystallites calculated using Scherrer formula is 8.2 nm. It is obvious that the real structure is formed from the above agglomerates of crystallites, leads to the formation of mesoporous structure which was confirmed by the isotherm adsorption-desorption of nitrogen and related to the type IV of IUPAC classification, characteristic of solids with the presence of mesopores (Fig. 1b) [28].

Type H1 hysteresis is inherent in cylindrical pores formed by agglomerates of spherical particles – globules with similar size, which are uniformly packed [29]. Specific surface area, calculated using one-point BET method was 14 m^2 g^{-1}, pore volume was 0.030 cm^3 g^{-1} and an

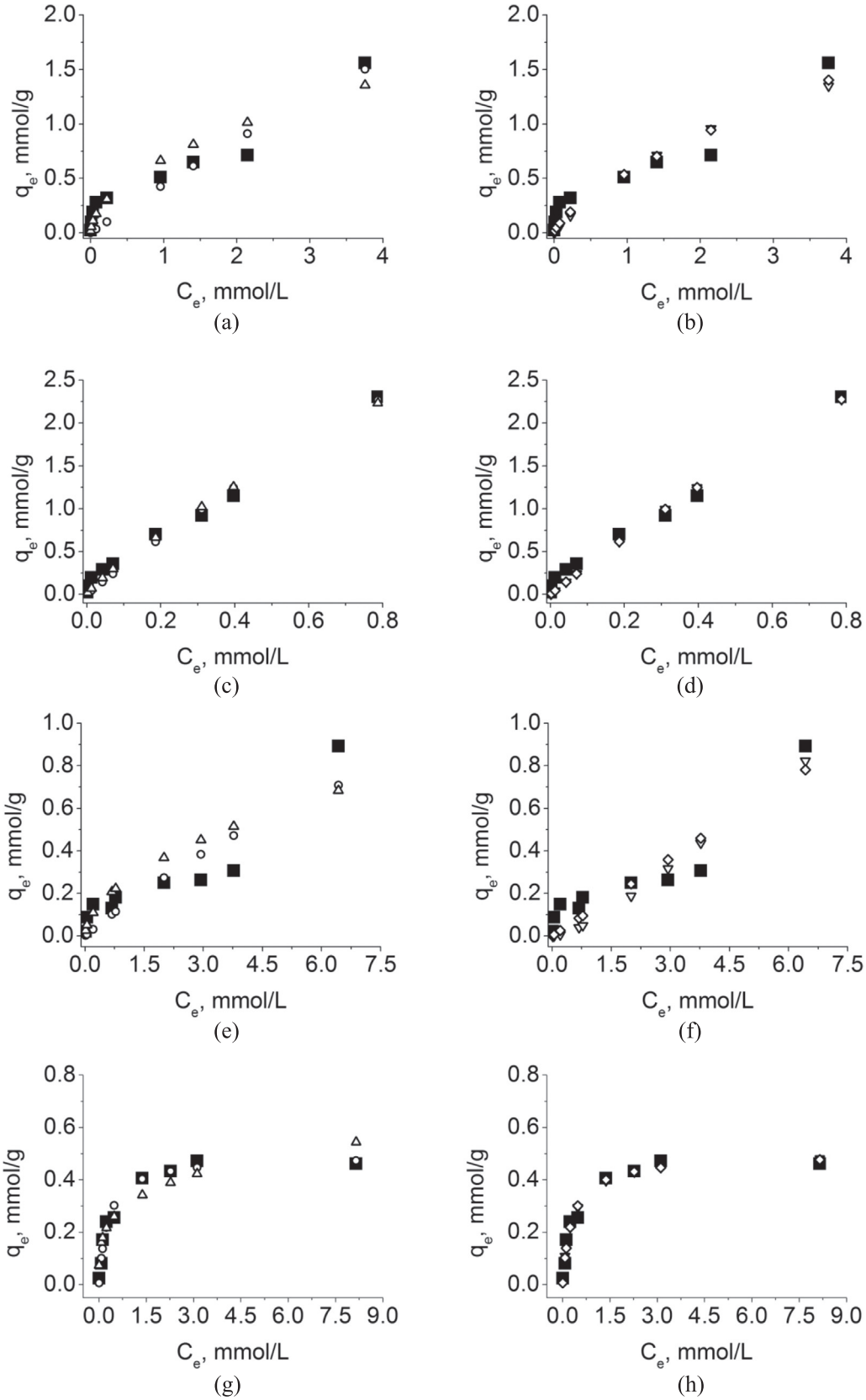

Fig. 5. Isotherms of metal ions sorption: (a, b) – Mn^{2+}, (c, d) – Co^{2+}, (e, f) Ni^{2+}, (g, h) – Cu^{2+} (pH = 5.0, contact time – 120 min).

Table 1
Isotherm parameters calculated from different sorption models.

	Mn^{2+}	Co^{2+}	Ni^{2+}	Cu^{2+}		Mn^{2+}	Co^{2+}	Ni^{2+}	Cu^{2+}
Langmuir					Freundlich				
q_m, mmol·g^{-1}	11.15	13.90	2.50	0.49	K_F, (mmol·g^{-1})/ (L·mmol$_F^{-1)n}$	0.68	2.73	0.25	0.31
K_L, L·mmol^{-1}	0.04	0.25	0.06	3.35	n_F	1.91	1.19	1.88	3.83
R^2	0.886	0.979	0.807	0.977	R^2	0.886	0.985	0.722	0.892
q_e exp, mmol·g^{-1}	1.56	2.30	0.89	0.46	q_e exp, mmol·g^{-1}	1.56	2.30	0.89	0.46
q_e calc, mmol·g^{-1}	1.50	2.27	0.71	0.47	q_e calc, mmol·g^{-1}	1.36	2.23	0.68	0.54
Sips					Redlich-Peterson				
q_m, mmol·g^{-1}	3.50	13.92	3.20	0.51	K_{RP}, L·mmol^{-1}	2704	3.45	0.12	1.71
K_S, (mmol·L^{-1})$_S^{-1/n}$	0.19	0.25	0.02	2.64	a_{RP}, (mmol·L^{-1})$^{-g}$	4885	0.25	0.001	3.57
n_S	1.10	1.00	0.68	1.13	g	0.30	0.99	0.99	0.99
R^2	0.875	0.979	0.844	0.980	R^2	0.907	0.980	0.854	0.977
q_e exp, mmol·g^{-1}	1.56	2.30	0.89	0.46	q_e exp, mmol·g^{-1}	1.56	2.30	0.89	0.46
q_e calc, mmol·g^{-1}	1.35	2.28	0.82	0.48	q_e calc, mmol·g^{-1}	1.40	2.28	0.78	0.48

Table 2
Comparison of Mn^{2+}, Co^{2+}, Ni^{2+} and Cu^{2+} adsorption on magnetic nanoparticles $MgFe_2O_4$ with other absorbents.

Adsorbent	Pollutant	Synthesis method	r, nm	Dose, g·L^{-1}	C_o, mg L^{-1}	Contact time	q_e, mmol·g^{-1}	Reference
n-$MgFe_2O_4$	Co^{2+}	Chemical precipitation	25–35	6.0	500	90 min	1.1	[24]
Chitosan- $MnFe_2O_4$	Cu^{2+}	Microwave-assisted hydrothermal method	100	3.3	1000	8 h	1.0	[33]
3D porous $NiFe_2O_4$	Cu^{2+}	Sol-gel	–	–	200	–	0.88	[31]
	Ni^{2+}	method					0.63	
Fe_3O_4	Mn^{2+}	Co-precipitation	< 10	4.0	150	24 h	0.14	[32]
	Cu^{2+}						0.17	
$MgFe_2O_4$	Mn^{2+}	Glycine-nitrate method	13–25	4.0	549	2 h	1.56	This work
	Co^{2+}				589		2.30	
	Ni^{2+}				587		0.89	
	Cu^{2+}				636		0.46	

Table 3
Sorption capacity and metal ions concentration during $MgFe_2O_4$ sorbent regeneration by $MgCl_2$ solutions of different concentrations.

Regeneration solution	Metal ion	$q_{initial}$, mmol·g^{-1}	q_{reg}, mmol·g^{-1}	$q_{initial}/q_{reg}$	C(Fe^{3+}), mg·L^{-1}	C(Mg^{2+}), mg·L^{-1}
10^{-1} M $MgCl_2$	Mn^{2+}	1.56	1.59	1.02	0.29	376.7
	Co^{2+}	2.30	2.31	1.00	1.15	378.4
	Ni^{2+}	0.89	1.06	1.19	0.51	380.0
	Cu^{2+}	0.46	1.06	2.30	0.91	377.1
10^{-2} M $MgCl_2$	Mn^{2+}	1.56	1.57	1.00	0.52	171.2
	Co^{2+}	2.30	2.31	1.00	0.50	172.4
	Ni^{2+}	0.89	1.09	1.22	0.70	172.8
	Cu^{2+}	0.46	1.06	2.30	2.19	171.0
10^{-3} M $MgCl_2$	Mn^{2+}	1.56	1.65	1.06	2.31	31.8
	Co^{2+}	2.30	2.32	1.01	4.51	37.6
	Ni^{2+}	0.89	1.22	1.36	1.91	35.2
	Cu^{2+}	0.46	1.06	2.30	3.11	36.9

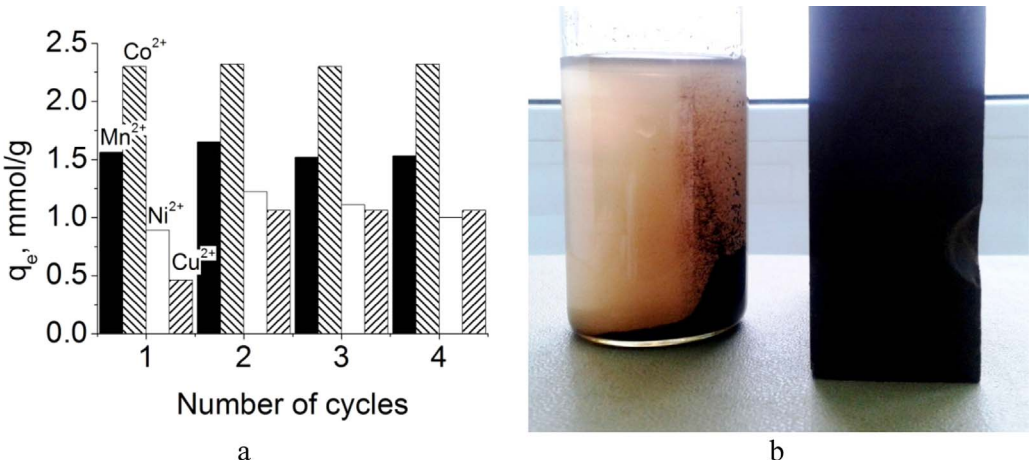

Fig. 6. Sorption capacity of $MgFe_2O_4$ after regeneration by 10^{-3} M $MgCl_2$ (a) and photo of $MgFe_2O_4$ nanoparticles in aqueous solution after 15 min in magnetic field (b).

average pore size was 8 nm. Fig. 1c shows that the $MgFe_2O_4$ sample consists of spherical agglomerates with sizes below 1 μm, composed of primary particles (crystallites) with a size of 21.2 nm (Fig. 1d). It is known that the calculation of the Scherer formula underestimates the result, as the peak broadening observed on the X-ray is associated not only with particle size, but also with other parameters and, in particular, with the distortions and lattice defects.

3.2. Effect of metal ion concentration and contact time

Fig. 2 shows the effect of initial metal ion concentrations and contact time on the removal efficiency of Mn^{2+}, Co^{2+}, Ni^{2+} and Cu^{2+} ions. Thus, in the whole investigated range of C_0 for Co^{2+}, high removal efficiency was observed (90–100%). It is important to note that regardless of the initial concentration of Co^{2+}, removal efficiency didn't change after a contact time of 10 min, which indicates a high rate of sorption equilibrium.

For the other cations, the removal efficiency decreased with increasing the initial concentration of Mn^{2+}, Co^{2+} and Ni^{2+} up to $C_0 = 5 \times 10^{-2}$–10^{-2} M. During sorption from solutions with low concentrations (10^{-4} – 10^{-3} M) the maximum removal efficiency was reached within 20–60 min, while at high C_0 (5×10^{-2} – 10^{-2} M), the time to reach equilibrium was reduced to 10–20 min and the removal efficiency does not change significantly in the interval up to 90 min.

Thus, to increase the affinity of the sorbent for metal ions they can be arranged in the following range of Co^{2+} (r = 0,72 Å) > Mn^{2+} (r = 0,80 Å) > Ni^{2+} (r = 0,69 Å) > Cu^{2+} (r = 0,73 Å). This result is not consistent with the change of ionic radius r of the extracted cations, which indicates that a complex mechanism of adsorption appears to be a combination of the surface complexation, electrostatic interaction and ion exchange processes. For further experiments on the effect of pH and the conditions of regeneration of the sorbent, 0.01 M initial concentration was chosen for all metal ions.

3.3. Effect of pH

Fig. 3 shows the effect of pH on the removal efficiency of metal ions. The increase in pH slightly affected the removal efficiency. Thus, the maximum sorption capacity of Mn^{2+}, Co^{2+}, Ni^{2+} and Cu^{2+} ions was 1.56, 2.30, 0.89 and 0.46 mmol g^{-1}, respectively. The value of removal efficiency of these cations varies considerably and ranges from 18% to 92% depending on the metal ions.

Adsorption of any ion types depends on the nature of the surface of the adsorbent and the speciation data of ions in solution at different pH values. The surface charge of the sorbent can be described by pH of point of zero charge (pH_{pzc}). In the case when pH < pH_{pzc} then the surface is dominated by excess of positive charge and the sorbent behaves like a Branstad acid. At pH > pH_{pzc} the sorbent will act as a Branstad base. Interacting with water, ferrites with a spinel structure form on the S-OH, surface layer which are capable of reacting with ions [30].

Fig. 4 shows that for $MgFe_2O_4$, pH_{pzc} is 6,58 - thus, at pH < pH_{pzc}, the surface is charged positively (Eq. (8)) and the sorption of Mn^{2+}, Co^{2+}, Ni^{2+}, Cu^{2+} ions can be described by Eq. (9). So, pH does not affect the sorption capacity in the range of 3.0–7.0. It is in good agreement with a high value of pH_{pzc} for studied $MgFe_2O_4$ sorbent.

$$S - OH_{(surf)} + H^+_{(aq)} \rightleftarrows S - OH^+_{2(surf)} \quad (8)$$

$$S - OH^+_{2(surf)} + Me^{2+}_{(aq)} \rightleftarrows S - OMe^+_{(surf)} + 2H^+_{(aq)} \quad (9)$$

3.4. Sorption isotherms modeling

Fig. 5 shows sorption isotherms of Mn^{2+}, Co^{2+}, Ni^{2+}, Cu^{2+} metal ions on the $MgFe_2O_4$ sorbent. Isotherms presented in Fig. 5 refer to H- or L-type according to the Giles classification. In the initial stages of interaction, $MgFe_2O_4$ exhibits a greater affinity for the metal ions. With the increase of solution concentration, the ratio between the concentrations of the remaining ions in solution and the ones adsorbed by the sorbent decreases, resulting in the isotherm becoming a straight line. The decrease in slope is due to the fact, that the adsorbed ions form a flat layer on the $MgFe_2O_4$ surface and excess ions are unable to find free sites for adsorption.

From the calculated parameters of sorption isotherms (Table 1), it follows that the sorption of Co^{2+} and Cu^{2+} ions onto $MgFe_2O_4$ can be reliably described by the equation of the monomolecular Langmuir adsorption. The values of q_{ecalc} for these metals, calculated from the Langmuir model equation, are close to q_{eexp} and the R^2 approximation coefficients equal 0.979 and 0.977 for Co^{2+} and Cu^{2+}, respectively. The Sips and Redlich-Peterson models also adequately describe the data sorption isotherms, and the n_S and g exponents are close to 1.00. This phenomenon confirms the closeness to the Langmuir equation. Thus, it makes sense to calculate the equilibrium parameter R_L. The Co^{2+} parameter R_L for all initial concentrations is close to 1.00 and the Freundlich equation exponent n_F is also close to 1.00 and equal to 1.19. From this, it follows that the isotherm takes a flat shape, as confirmed by Fig. 5c,d. For the Cu^{2+} parameter, R_L being close to 1.00, however, the Freundlich exponent much exceeds the value of 1.00 and equals 3.83, i.e., the isotherm takes a non-flat shape.

From Table 1 it is seen that for low values of the R^2 approximation coefficients not exceeding 0.900, sorption isotherms of Mn^{2+} and Ni^{2+} ions cannot be described by any of the above models of sorption. A comparative study of sorption capacity of synthesized $MgFe_2O_4$ nanoparticles and other magnetic sorbents is shown in Table 2. The synthesized nanoparticles have significant sorption capacity for Mn^{2+}, Co^{2+}, Ni^{2+} and Cu^{2+} and can be efficiently used for the water treatment.

3.5. Regeneration study

One of the most important characteristics of sorbents is the possibility of their regeneration, which can be used for multiple wastewater treatments. Given the composition of $MgFe_2O_4$ magnetic sorbent and proposed mechanism of metal ions sorption, including surface complexation, electrostatic interaction and ion exchange, we have suggested the possibility of sorbent regeneration with $MgCl_2$ solutions. As shown in Table 3, the regeneration of the sorbent can be performed under mild conditions without the use of acids, leading to the formation of acidic wastewater that requires subsequent neutralization and disposal. For all the studied metals $q_{reg}/q_{init} > 1$, which indicates that the sorption characteristics of $MgFe_2O_4$ sorbent are completely recovered.

It is important to note that at high concentrations (10^{-1}–10^{-2}M) of the $MgCl_2$ regeneration solution, there is a high residual concentration of Mg^{2+} ions in stock solution. Regardless of the conditions of regeneration of the $MgFe_2O_4$ sorbent, the concentration of Fe^{3+} ions in the stock solution is insignificant and was in the range of 0.19–4.51 mg L^{-1}, which indicates the stability of the sorbent and no changes to its structure in the regeneration process. Thus, it is advisable to use a solution of 10^{-3} M $MgCl_2$ for sorbent regeneration from the point of view of $MgCl_2$ consumption and minimize the residual concentration of Mg^{2+} ions in the stock solution.

Study on 4 cycles of sorption for Mn^{2+}, Co^{2+}, Ni^{2+} ions with the subsequent $MgFe_2O_4$ regeneration by 10^{-3} M $MgCl_2$ solution showed the reusability of the sorbent with the restoration of its capacity up to 100 ± 5% (Fig. 6a). It was observed that regenerated sorbent gave increased removal efficiency for Cu^{2+} ions which may be due to enhancement of surface adsorption site, which was not available in bare adsorbent due to agglomerated particles and after regeneration with $MgCl_2$, those blocked sites exposed for interaction with Cu^{2+} ions. This phenomenon is poorly described in the literature [34] and requires further study. Also after repeated $MgFe_2O_4$ regeneration, preservation of their magnetic properties was found (Fig. 6b).

4. Conclusions

Magnetic magnesium ferrite was synthesized using modified glycine-nitrate method when high temperature inert component (NaCl) was injected to create "protected" and not aggregated nanoparticles. The obtained $MgFe_2O_4$ nanoparticles were characterized by a low degree of crystallinity (crystallite size of 8.2 nm), mesoporous structure (A_{BET} of 14 $m^2\ g^{-1}$, V_{BJH} of 0.030 $cm^3\ g^{-1}$ and D_{BJH} of 8 nm), and were presented in the form of spherical agglomerates with a size of about 1 μm consisting of crystallite 13–25 nm in size. Following trend $Co^{2+} > Mn^{2+} > Ni^{2+} > Cu^{2+}$ was observed for the sorption of metal ions. The maximum sorption capacity of Mn^{2+}, Co^{2+}, Ni^{2+} and Cu^{2+} ions at pH = 5.0 were 1.56, 2.30, 0.89 and 0.46 mmol g^{-1} respectively. Regardless of the initial concentration, removal efficiency of metal ions remains essentially unchanged after 20–60 min of contact with the sorbent. No significant effect of pH was observed in the studied range 3.0–7.0 due to high value of pH_{pzc} $MgFe_2O_4$. The sorption of Co^{2+} and Cu^{2+} ions onto $MgFe_2O_4$ can be reliably described by the equation of monomolecular Langmuir adsorption. The sorption of Mn^{2+} and Ni^{2+} ions cannot be described by any of the studied sorption models. Conducting four cycles of sorption with the subsequent $MgFe_2O_4$ regeneration by 10^3 M $MgCl_2$ solution showed the reusability of the sorbent.

Acknowledgments

This work was partly financially supported by the Belarusian Republican Foundation for Fundamental Research (grant # Х17УКРГ – 001).

References

[1] A.E. Burakov, E.V. Galunin, I.V. Burakova, A.E. Kucherova, S. Aqarwal, A.G. Tkachev, V.K. Gupta, Adsorption of heavy metals on conventional and nanostructured materials for wastewater treatment purposes: a review, Ecotoxicol. Environ. Saf. 148 (2018) 702–712, http://dx.doi.org/10.1016/j.ecoenv.2017.11.034.

[2] D. Mehta, S. Mazumbar, S.K. Singh, Magnetic adsorbents for the treatment of water/wastewater, J. Water Process Eng. 7 (2015) 244–265, http://dx.doi.org/10.1016/j.jwpe.2015.07.001.

[3] M. Naghdi, M. Taheran, S.K. Brar, A. Kermanshahi-Pour, M. Verma, R.Y. Surampali, Removal of pharmaceutical compounds in water and wastewater using fungal oxidoreductase enzymes, Environ. Pollut. 234 (2018) 190–213, http://dx.doi.org/10.1016/j.envpol.2017.11.060.

[4] D. Mehta, S. Mazumdar, S.K. Singh, Magnetic adsorbents for the treatment of water/wastewater – A review, J. Water Process Eng. 7 (2015) 244–265, http://dx.doi.org/10.1016/j.jwpe.2015.07.001.

[5] D. Lucas, et al., The role of sorption processes in the removal of pharmaceuticals by fungal treatment of wastewater, Sci. Total Environ. 610–611 (2018) 1147–1153.

[6] E. Da'na, A. Awad, Regeneration of spent activated carbon obtained from home filtration system and applying it for heavy metals adsorption, J. Environ. Chem. Eng. 5 (4) (2017) 3091–3099, http://dx.doi.org/10.1016/j.jece.2017.06.022.

[7] T. Kameda, Y. Suzuki, T. Yoshioka, Removal of arsenic from an aqueous solution by coprecipitation with manganese oxide, J. Environ. Chem. Eng. 2 (4) (2014) 2045–2049, http://dx.doi.org/10.1016/j.jece.2014.09.004.

[8] A.J. Hargreaves, P. Vale, J. Whelan, L. Alibardi, C. Constantino, G. Dorto, E. Cartmell, P. Campo, Impacts of coagulation-flocculation treatment on the size distribution and bioavailability of trace metals (Cu, Pb, Ni, Zn) in municipal wastewater, Water Res. 128 (1) (2018) 120–128, http://dx.doi.org/10.1016/j.watres.2017.10.050.

[9] P.S. Goh, A.F. Ismail, A review on inorganic membranes for desalination and wastewater treatment, Desalination (2017), http://dx.doi.org/10.1016/j.desal.2017.07.023.

[10] T. Tuutijärvi, R. Vahala, M. Sillanpää, G. Chen, Maghemite nanoparticles for As(V) removal: desorption characteristics and adsorbent recovery, Environ. Technol. 33 (16) (2012) 1927–1936, http://dx.doi.org/10.1080/09593330.2011.651162.

[11] S. Hokkanen, E. Repo, S. Lou, M. Sillanpää, Removal of arsenic(V) by magnetic nanoparticle activated microfibrillated cellulose, Chem. Eng. J. 260 (15) (2015) 886–894, http://dx.doi.org/10.1016/j.cej.2014.08.093.

[12] D.L. Ramasamy, V. Puhakka, E. Repo, M. Sillanpää, Selective separation of scandium from iron, aluminium and gold rich wastewater using various amino and non-amino functionalized silica gels – A comparative study, J. Clean. Prod. 170 (2018) 890–901, http://dx.doi.org/10.1016/j.jclepro.2017.09.199.

[13] A. Gürses, C. Dogar, M. Yalcin, M. Acikyildiz, R. Bayrak, S. Karaca, The adsorption kinetics of the cationic dye, methylene blue, onto clay, J. Hazard. Mater. 131 (1 – 3) (2016) 217–228, http://dx.doi.org/10.1016/j.jhazmat.2005.09.036.

[14] K. Sun, Y. Shi, X. Wang, Z. Li, Sorption and retention of diclofenac on zeolite in the presence of cationic surfactant, J. Hazard. Mater. 323 (A) (2017) 584–592, http://dx.doi.org/10.1016/j.jhazmat.2016.08.026.

[15] D. Czarna, P. Baran, P. Kunecki, R. Panek, R. Zmuda, M. Wdowin, Synthetic zeolites as potential sorbents of mercury from wastewater occurring during wet FGD processes of flue gas, J. Clean. Prod. (2017), http://dx.doi.org/10.1016/j.jclepro.2017.11.147.

[16] C.-G. Lee, M.-K. Song, J.-C. Ryu, C. Park, J.-W. Choi, S.-H. Lee, Application of carbon foam for heavy metal removal from industrial plating wastewater and toxicity evaluation of the adsorbent, Chemosphere 153 (2016) 1–9, http://dx.doi.org/10.1016/j.chemosphere.2016.03.034.

[17] N.M. Mahmoodi, M. Ghezelbash, M. Shabanian, F. Aryanasab, M.R. Saeb, Efficient removal of cationic dyes from colored wastewaters by dithiocarbamate-functionalized graphene oxide nanosheets: from synthesis to detailed kinetics studies, J. Taiwan Inst. Chem. Eng. 81 (2017) 239–246, http://dx.doi.org/10.1016/j.jtice.2017.10.011.

[18] M.A. Mahmoad, Kinetics and thermodynamics of aluminum oxide nanopowder as adsorbent for Fe (III) from aqueous solution. Beni-Suef Univ, J. Appl. Sci. 4 (2) (2015) 142–149, http://dx.doi.org/10.1016/j.bjbas.2015.05.008.

[19] A.I. Ivanets, V.G. Prozorovich, T.F. Kouznetsova, A.V. Radkevich, A.M. Zarubo, Mesoporous manganese oxides prepared by sol-gel method: synthesis, characterization and sorption properties towards strontium ions, Environ. Nanotechnol.,Monit. Manag. 6 (2016) 261–269, http://dx.doi.org/10.1016/j.enmm.2016.11.004.

[20] A.M.A. Morsy, Performance of magnetic talc titanium oxide composite for thorium ions adsorption from acidic solution, Environ. Technol. Innov. 8 (2017) 399–410, http://dx.doi.org/10.1016/j.eti.2017.09.004.

[21] C. Tokoro, Mechanism investigation and surface complexation modeling of zinc sorption on aluminum hydroxide in adsorption/coprecipitation processes, Chem. Eng. J. 279 (2015) 86–92, http://dx.doi.org/10.1016/j.cej.2015.05.003.

[22] V. Srivastava, T. Kohout, M. Sillanpää, Potential of cobalt ferrite nanoparticles (CoFe2O4) for remediation of hexavalent chromium from synthetic and printing press wastewater, J. Environ. Chem. Eng. 4 (3) (2016) 2922–2932, http://dx.doi.org/10.1016/j.jece.2016.06.002.

[23] L. Wang, J. Li, Y. Wang, L. Zhao, Q. Jiang, Adsorption capability for Congo red on nanocrystalline MFe_2O_4 (M = Mn, Fe, Co, Ni) spinel ferrites, Chem. Eng. J. 181–182 (2012) 72–79, http://dx.doi.org/10.1016/j.cej.2011.10.088.

[24] D.H.K. Reddy, Y.-S. Yun, Spinel ferrite magnetic adsorbents: alternative future materials for water purification? Coord. Chem. Rev. 315 (2016) 90–111, http://dx.doi.org/10.1016/j.ccr.2016.01.012.

[25] V. Srivastava, Y.C. Sharma, M. Sillanpää, Application of nano-magnesso ferrite (n-$MgFe_2O_4$) for the removal of Co^{2+} ions from synthetic wastewater: kinetic, equilibrium andthermodynamic studies, Appl. Surf. Sci. 338 (2015) 42–54, http://dx.doi.org/10.1016/j.apsusc.2015.02.072.

[26] D. Gusain, V. Srivastava, V.K. Singh, Y.C. Sharma, Crystallite size and phase transition demeanor of ceramic steel, Mater. Chem. Phys. 145 (3) (2014) 320–326, http://dx.doi.org/10.1016/j.matchemphys.2014.02.015.

[27] K.R. Hall, L.C. Eagleton, A. Acrivos, T. Vermeulen, Pore- and solid-diffusion kinetics in fixed-bed adsorption under constant-pattern conditions, Ind. Eng. Chem. Fundam. 5 (2) (1966) 212–223.

[28] M. Thommes, Physisorption of gases, with special reference to the evaluation of surface area and pore size distribution (IUPAC Technical Report), Pure Appl. Chem. 87 (9–10) (2015) 1051–1069, http://dx.doi.org/10.1515/ci-2016-0119.

[29] S.J. Gregg, K.S.W. Sing, Adsorption, Surface Area and Porosity, second ed., Academic Press, London, 1982.

[30] E. McCafferty, Acid-Base Properties of Surface Oxide Films, in Surface Chemistry of Aqueous Corrosion Processes, Springe. Int. Publ. (2015) 1–54, http://dx.doi.org/10.1007/978-3-319-15648-4_1.

[31] Y. Meng, D. Chen, Y. Sun, D. Jiao, D. Zeng, Z. Liu, Adsorption of Cu^{2+} ions using chitosan-modified magnetic Mn ferrite nanoparticles synthesized by microwave-assisted hydrothermal method, Appl. Surf. Sci. 324 (1) (2015) 745–750, http://dx.doi.org/10.1016/j.apsusc.2014.11.028.

[32] X. Hou, J. Feng, X. Liu, Y. Ren, Z. Fan, T. Wei, J. Meng, M. Zhang, Synthesis of 3D porous ferromagnetic $NiFe_2O_4$ and using as novel to treat wastewater, J. Colloid Interface Sci. 362 (2011) 477–485, http://dx.doi.org/10.1016/j.jcis.2011.06.070.

[33] L. Giraldo, A. Erto, J.C. Moreno-Pirajan, Magnetite nanoparticles for removal of heavy metals from aqueous solution: synthesis and characterization, Adsorption 19 (2–4) (2013) 465–474, http://dx.doi.org/10.1007/s10450-012-9468-1.

[34] Y.N. Mata, M.L. Blazquez, A. Ballester, F. Gonzalez, J.A. Munoz, Studies on sorption, desorption, regeneration and reuse of sugar-beet pectin gels for heavy metal removal, J. Hazard. Mater. 178 (1–3) (2010) 243–248, http://dx.doi.org/10.1016/j.jhazmat.2010.01.069.